Carbohydrate Polymers 95 (2013) 161–166

Contents lists available at SciVerse ScienceDirect

Carbohydrate Polymers

journal homepage: www.elsevier.com/locate/carbpol

# Interrelationship between the zeta potential and viscoelastic properties in coacervates complexes

Hugo Espinosa-Andrews[a,*], Karina Esmeralda Enríquez-Ramírez[a], Eristeo García-Márquez[b], Cesar Ramírez-Santiago[c], Consuelo Lobato-Calleros[c], Jaime Vernon-Carter[b]

[a] Unidad de Tecnología Alimentaria, Centro de Investigación y Asistencia en Tecnología y Diseño del Estado de Jalisco, A.C. Av. Normalistas #800, Guadalajara, Jalisco 44270, México
[b] Departamento de Ingeniería de Procesos e Hidráulica, Universidad Autónoma Metropolitana – Iztapalapa, San Rafael Atlixco # 186, México, D.F. 09340, México
[c] Departamento de Preparatoria Agrícola and Departamento de Ingeniería Agroindustrial, Universidad Autónoma Chapingo, Km. 38.5 Carretera México – Texcoco, Texcoco, Edo. México 56230, México

ARTICLE INFO

*Article history:*
Received 26 December 2012
Received in revised form 7 February 2013
Accepted 26 February 2013
Available online 5 March 2013

*Keywords:*
Gum Arabic
Chitosan
Polyelectrolytes
Complex coacervation
Zeta-potential
Rheology

ABSTRACT

The formation of the complex coacervate (CC) phases between gum Arabic (GA) and low molecular weight chitosan (Ch) and the interrelationship between the zeta-potential and viscoelastic properties of the coacervate phase were investigated. The maximum charge difference of biopolymers stock dispersion was displayed in a range of pH between 4.0 and 5.5. Titration experiment between the oppositely charged biopolymers showed that the isoelectric point was found at a biopolymers mass ratio ($R_{[GA:Ch]}$) of $R_{[5.5:1]}$. Turbidity, size and $\zeta$-potential of the soluble complexes (SC) showed an interrelation with the complex coacervate yield (CCY). Higher CCY values (82.2–88.1%) were obtained in the range from $R_{[3:1]}$ to $R_{[5.5:1]}$. Change the $R_{[GA:Ch]}$ in dispersion, make possible to produce CC's phases exhibiting cationic ($R_{[1:1]}$ and $R_{[3:1]}$), neutral ($R_{[5.5:1]}$) or anionic ($R_{[9:1]}$ and $R_{[7:1]}$) charged. All CC's exhibited liquid-viscoelastic behavior at lower frequencies and a crossover between $G''$ and $G'$ at higher frequencies.



## 1. Introduction

Biopolymer–biopolymer interactions play an increasingly important role in modern-day researches in food science and biotechnology because they influence the microstructure formation of most biopolymer-containing systems, determining in great extent their texture, mechanical stability, consistency and, ultimately, appearance and taste (Semenova, 2007). In order to achieve a desired functionality (e.g., emulsifying, texture or film properties) in a product, a greater understanding of the factors affecting biopolymers interactions is required, particularly those of electrostatic origin. Attractive interactions between two biopolymers can become evident in various ways: (i) formation of small soluble complex (SC), manifesting itself in murky solutions, (ii) formation of a homogeneous weak gel, if interactions are weak, and (iii) precipitation of both biopolymers, if interactions are strong (Walstra, 2003). The nature of these interactions may lead to either segregative or associative phase behavior, depending on biopolymer characteristics (e.g., charge density, size, type and distribution of reactive groups), biopolymer concentration and ratio, and solvent conditions (e.g., pH, temperature, ionic strength) (Espinosa-Andrews, Báez-González, Cruz-Sosa, & Vernon-Carter, 2007; Espinosa-Andrews, Sandoval-Castilla, Vázquez-Torres, Vernon-Carter, & Lobato-Calleros, 2010; Liu, Low, & Nickerson, 2010; Schatz et al., 2004; Singh et al., 2007).

Complex coacervation involves spontaneous separation into coexisting solvent-rich and solvent-depleted phase, the latter consisting of a co-precipitate of both biopolymers (Dickinson, 1995). Complex coacervates (CC) have many applications in the fields of biotechnology, pharmaceutical and food industry and its specific application will depend on their structure and rheological properties (Espinosa-Andrews et al., 2010). For example, one of the main applications of the electrostatic complexes is in the stabilization of emulsions and in the formation of wall materials of microcapsules for obtaining enhanced functional properties (Pérez-Orozco, Barrios-Salgado, Román-Guerrero, & Pedroza-Islas, 2011). Recently, in the field of food science, Ramírez-Santiago, Lobato-Calleros, Espinosa-Andrews, & Vernon-Carter (2012) reported that it is possible to formulate reduced-fat

* Corresponding author. Tel.: +52 333345 5200; fax: +52 333345 5200 1001.
*E-mail addresses:* hespinosa@ciatej.net.mx, andrewshugo@hotmail.com (H. Espinosa-Andrews).

0144-8617/$ – see front matter © 2013 Elsevier Ltd. All rights reserved.
http://dx.doi.org/10.1016/j.carbpol.2013.02.053

Petit-Suisse cheeses where milk cream (i.e., milk fat globules) was partially substituted by a whey protein isolate–low-methoxyl pectin CC, displaying dynamic rheological properties and overall sensory acceptability similar to that of a full-fat Petit-Suisse cheese. Nevertheless, the key to moving further in the field of practical applications is to redouble efforts in the investigation of the structures and physicochemical characteristics of the CC.

The objective of this work was to determine the conditions leading to the formation of the complex coacervate between gum Arabic-low molecular weight chitosan and to establish an interrelationship between the zeta potential and viscoelastic properties of the coacervate phase.

## 2. Material and methods

### 2.1. Materials

Low molecular weight chitosan, (Ch; 92.2% degree of deacetylation, DDA) was purchased from Sigma–Aldrich (St. Louis, MO, USA). Ch (1–300 kDa) is a cationic heterogeneous binary polysaccharide that consists primarily of 2-acetamido-2-deoxy-$\beta$-D-glucopyranose and 2-amino-2-deoxy-$\beta$-D-glucopyranose residues (Claesson & Ninhami, 1992); is produced by chemical, thermal, or biochemically degradation of high molecular weight chitosan (Niederhofer & Müller, 2004). The techno-functional applications of Ch are principally as a drug carrier for delivery systems (Park, Saravanakumar, Kim, & Kwon, 2010), emulsion stabilizer (Klinkesorn & Namatsila, 2009) or as a barrier material (Hernández-Ochoa, Gonzales-Gonzales, Gutiérrez-Mendez, Muñoz-Castellanos, & Quintero-Ramos, 2011). Gum Arabic (GA; *Acacia senegal*) tear drops was purchased from Natural Products (Yautepec, State of Morelos, Mexico). GA is a branched, neutral or slightly acidic, complex polysaccharide obtained as mixed calcium, magnesium and potassium salts (Renard, Lavenant-Gourgeon, Ralet, & Sanchez, 2006). Studies on the structure of GA indicate that the molecules consist of a $\beta$ $(1\rightarrow3)$ linked galactopyranose backbone chain with numerous branches linked through $\beta$ $(1\rightarrow6)$ galactopyranose residues and containing arabinofuranose, arabinopyranose, rhamnopyranose, glucuronic acid and 4-*O*-methyl-D-glucuronic acid, with small amount of proteinaceous material as an integral part of the structure (Espinosa-Andrews et al., 2008). Acetic acid (AA), hydrochloric acid (HCl) and sodium hydroxide (NaOH) were purchased from J.T. Baker (Xalostoc, State of Mexico, Mexico).

### 2.2. Stock dispersions

Stock dispersions of both polysaccharides were prepared by dispersing Ch (3 wt%) in deionized water with acetic acid (1%, v/v) and the GA tear drops were pulverized, dissolved in deionized water and filtered for preparing a 10 wt% dispersion. Both stock dispersions were gently stirred for 12 h and stored overnight at 4 °C to ensure complete hydration of the biopolymers.

### 2.3. Zeta ($\zeta$) potential of stock dispersions

The $\zeta$-potential was determined using the Zetasizer Nano ZS90 equipment (Malvern Instruments, Worcestershire, UK). The stock dispersions were diluted to a concentration of approximately 0.01 wt% using deionized water prior to analysis. Diluted polysaccharides dispersions (10 mL) were transferred to an autotitrator MPT-2 (Malvern Instruments, Worcestershire, UK) to adjust the pH of the dispersions using either 0.1 N HCl or 0.1 N NaOH. Experiments were performed at pH ranging from 2 to 7 every 0.5 units with a pH resolution of $\pm$0.05 units. The $\zeta$-potential was determined by measuring the direction and velocity of the biopolymers dispersion as they moved along the applied electric field. The equipment software converted the electrophoretic mobility measurements into $\zeta$-potential values using the Smoluchowsky mathematical model.

Dilutions of 0.2 mg mL$^{-1}$ of Ch and 5 mg mL$^{-1}$ of GA were prepared in order to carry a titration experiment between the oppositely charged biopolymers. Ch (10 mL) was transferred to the autotitrator MPT-2 at pH of 4.5. Then, the GA was added above the isoelectric point of the mixture. At the same time the size distributions of the GA/Ch aggregates were determined using the Zetasizer Nano ZS90 by plotting the *z*-average radius ($R_h$) as a function of anionic polysaccharide (GA) addition. The $R_h$ was calculated using the Stokes–Einstein equation: $R_h = k_B T/6\pi\eta_s D$; where $k_B$ is the Boltzmann constant, $T$ is the absolute temperature, $\eta_s$ is the dynamic viscosity of the solvent and $D$ is the *z*-average translational diffusion coefficient. The titration measurements are reported as the average $\pm$ standard deviation of measurements made on three independent samples with three measurements made per run at 20 °C.

### 2.4. Preparation of biopolymers mixtures

Based on the titration experiment between the oppositely charged biopolymers, five different weight biopolymers mass ratio ($R_{[GA:Ch]}$) at 5% (w/w) of total biopolymers weight concentrations were made ($R_{[1:1]}$, $R_{[3:1]}$, $R_{[5.5:1]}$, $R_{[7:1]}$ and $R_{[9:1]}$), by mixing the requisite amount of both stock dispersions at a constant pH value of 4.5 (Espinosa-Andrews et al., 2007). The dispersions were left to rest at 20 °C and turbidity and electrophoretic measurements were taken daily until two consecutive readings were equal (usually between 5 and 7 days). Complete separation of the precipitated CC from the SC was achieved by centrifuging at 8000 rpm for 10 min.

### 2.5. Characterization of the biopolymers complexes

#### 2.5.1. Soluble complexes

The turbidity of the SC was characterized by measuring the optical density at $\lambda$ = 600 nm using a Cintra 6 UV–vis spectrophotometer (GBC Scientific Equipment Pty. Ltd., Braeside, VIC, Australia). At this wavelength both individual polyelectrolytes do not absorb light. Deionized water was used to establish the baseline (Espinosa-Andrews et al., 2007).

The $\zeta$-potential and the $R_h$ of the SC were measured using the Zetasizer Nano ZS90 equipment at 20 °C.

#### 2.5.2. Insoluble complexes

Complex coacervate yield (CCY) was determined using the following equation (Ramírez-Santiago et al., 2012).

$$\text{CCY} = \frac{\text{weight of CC in d.b.}}{\text{total weight of Ch} + \text{GA in the dispersion}} \times 100 \quad (1)$$

The $\zeta$-potential of the CC was measured as a function of pH. Approximately 0.3 g of the CC were put into 10 mL HCl (0.02 N) in order to decrease the pH of the CC's, shaken vigorously and stored for 24 h. The pH of the redispersed CC was adjusted with 0.1 N NaOH from 2 to 7 every 0.5 units with a pH resolution of $\pm$0.1 units, and the $\zeta$-potential was measured at the different pH values.

### 2.6. Rheological measurements

CC viscoelastic properties were determined with an AR1000 rheometer (TA Instruments, Newcastle, DE, USA) coupled to a truncated cone–plate geometry (1°, 60 mm diameter) with a gap of 0.029 mm between the flat surfaces of both elements at 5 °C (Espinosa-Andrews et al., 2010). This temperature was chosen for enhanced the sensibility of the measurements and to avoid sample evaporation. Amplitude strain sweeps (0.1–100%) were applied

under a constant angular frequency ($\omega$) of 6.25 rad $s^{-1}$ in order to determine the linear viscoelastic region (LVER), where the dynamic storage modulus ($G'$) and loss modulus ($G''$) are independent of strain. The oscillating sweep measurements were carried out over an extended $\omega$ domain of 0.1–100 rad $s^{-1}$ under the LVER.

### 2.7. Statistical analyses

All measurements were done by triplicate and reported as means ± standard deviations. Simple classification variance analysis was applied and, whenever it was appropriate, Tukey's test was used in order to determine differences between the means ($p < 0.05$). Statistical analyses were done with Statgraphics centurion XVI program version 16.1.17 (StatPoint Technologies, Inc., Warrenton, Virginia, USA).

## 3. Results and discussion

### 3.1. ζ-potential of stock dispersions

The ζ-potential variation with pH for the Ch and GA dispersions is shown in Fig. 1. Ch dispersions displayed a weak charged polyelectrolyte behavior, exhibiting positive ζ-potential values at all pH values studied, with the positive charge decreasing considerably as pH reached a value of 7.0. This phenomenon is commonly attributed to the loss charge of the glucosamine segments (p*Ka* 6.3–7.5) (Guzey and McClements, 2006; Hudson & Jenkins, 2001) and to the decrease of any electrostatic screening effects as increasing amounts of NaOH were added to neutralize dispersion pH (Helgason, Gislason, McClements, Kristbergsson, & Weiss, 2009). Ch conformation and its interaction with the solvent depend on the number of positive charges ($NH_3^+$) on its backbone, which in turn, depend on DDA, the pH and the ionic strength of the solvent. On the other hand, the GA dispersion exhibited negative ζ-potential values over the whole pH range, due to the pKa values of the carboxyl groups (1.8–2.2). The ζ-potential became increasingly negative as the dispersion pH increased from 2 to 7, reaching a maximum value (−25.7 ± 0.9 mV) at pH of 7.0. The GA ζ-potential values over the whole pH range studied were higher than those reported by Jiménez-Alvarado, Beristain, Medina-Torres, Román-Guerrero, & Vernon-Carter (2009) and Schmitt, Sanchez, Thomas, & Hardy (1999), but similar to those reported by Weinbreck, Tromp, & de Kruif (2004). These differences could be related by chemical composition variations of the polysaccharide exudates of *Acacia* spp. trees, which are dependent on the origin, type, age of tree, and season of gum harvesting. The strength of the electrostatic interaction (SEI) between oppositely charged polyelectrolytes can be calculated as the product of the absolute value of ζ-potential of both macromolecules at each pH values (Weinbreck et al., 2004). The highest SEI values indicate the range of pH where the attractions between opposite biopolymers could be strongest. The highest SEI values were found in a pH range between 4.0 and 5.0 (Fig. 1).

Fig. 2 shows the evolution of the ζ-potential and $R_h$ as the Ch dispersion (0.2 mg $mL^{-1}$) was titrated with the GA dispersion (5 mg $mL^{-1}$). The GA:Ch system was characterized by the progressive appearance of three important zones as the addition of the GA proceeded: (A) a region where the cationic polyelectrolyte (Ch) to anionic polyelectrolyte (GA) ratio was relatively low ($\sim R_{[0:1]} - R_{[4.5:1]}$), where both macromolecules associated weakly with each other to form SC. This region was characterized by a progressive decrease in the net charge of the system as the $R_{[GA:Ch]}$ increased. However, even at an $R_{[GA:Ch]}$ of [4.5:1] the net charge displayed by the system was relatively low (~20 mV), being insufficient for promoting the aggregation of SC. As a result of this, the $R_h$ of the complexes was relatively small (<125 nm) and

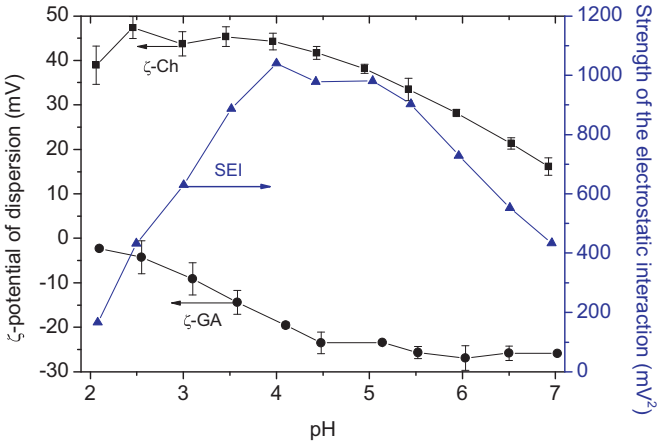


**Fig. 1.** ζ-potential of Ch(■) and GA(●) dispersions and strength of the electrostatic interaction of GA:Ch (▲) at different pH values.

remained almost constant (polydispersity index, PdI < 0.3). It is important to draw attention to the fact that at the beginning of the titration, the $R_h$ of the system decreased due to a spatial rearrangement of both biopolymers in dispersion; (B) an intermediate $R_{[GA:Ch]}$ region ($\sim R_{[4.5:1]} - R_{[6.5:1]}$) where the ζ-potential values of the GA–Ch dispersions underwent a drastic downward gradient change, characterized by a charge switchover from positive to negative values, accompanied by a sharp upward increase in the $R_h$ of the [GA:Ch] complexes due to aggregative phenomena which eventually led to the precipitation of the CC (PdI > 0.5). The isoelectric point occurred around a $R_{[GA:Ch]}$ of 5.5 ± 0.2 g of GA per g of Ch. A similar relationship have been reported for the system GA-medium molecular weight Ch (Espinosa-Andrews et al., 2007), suggesting that the molecular mass of the latter does not influence the relation of complexation; and (C) a region at relatively high [GA:Ch] ratio (>$R_{[6.5:1]}$), where the net charge of both systems did not change significantly (−24.5 mV), reaching similar values to those observed for GA alone, suggesting that Ch molecules were completely surrounded by GA molecules.

### 3.2. Biopolymers complexes characterization

The turbidity and ζ-potential data of the SC were used to tune the region and time where CC formation was achieved. CC formation was ensured for all the $R_{[GA:Ch]}$ after 7 days, so that after this time period they were separated by centrifugation and analyses

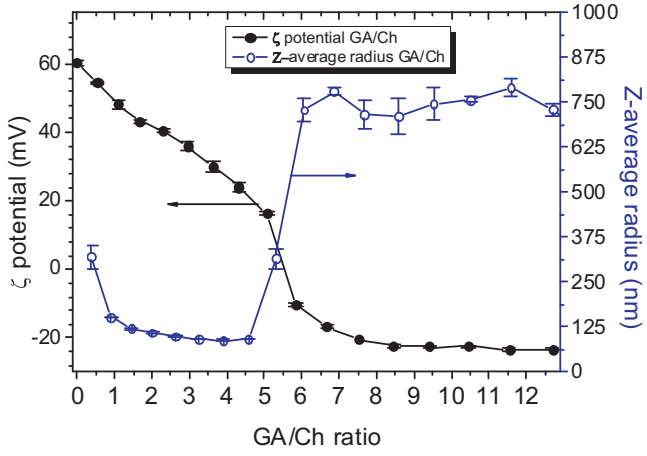


**Fig. 2.** Evolution of the ζ-potential (●) and *z*-average radius (○) as the cationic polyelectrolyte (Ch) was titrated with the anionic polyelectrolyte (GA).

**Table 1**
Interrelationship between complex coacervates yield and the turbidity, *z*-average ratio and ζ-potential of soluble complexes at different [GA:Ch] ratios.

| $R_{[GA:Ch]}$ | Turbidity | ζ-potential (mV) | $R_h$ (nm) | CCY (%) |
|---|---|---|---|---|
| [1:1] | 0.32 ± 0.04[a] | +34.2 ± 2.5[a] | 221.6 ± 3.0[a] | 45.4 ± 8.4[a] |
| [3:1] | 0.07 ± 0.04[a] | +15.6 ± 1.5[b] | 46.9 ± 21.3[b] | 82.6 ± 0.4[b] |
| [5.5:1] | 0.03 ± 0.02[a] | −10.7 ± 0.8[c] | 56.5 ± 15.1[b] | 85.9 ± 2.2[b] |
| [7:1] | 2.52 ± 0.36[b] | −17.2 ± 1.1[d] | 537.0 ± 3.7[c] | 58.2 ± 2.7[c] |
| [9:1] | 3.35 ± 0.23[c] | −19.4 ± 0.6[d] | 894.8 ± 47.6[d] | 41.9 ± 5.4[a] |

$R_{[GA:Ch]}$ = biopolymers ratio; CCY = complex coacervate yield; $R_h$ = *z*-average radius of biopolymers complex values are mean of three replicates ± standard error.
[a,b,c,d] Means in the same column with different lower case letters are significantly different ($P < 0.05$).

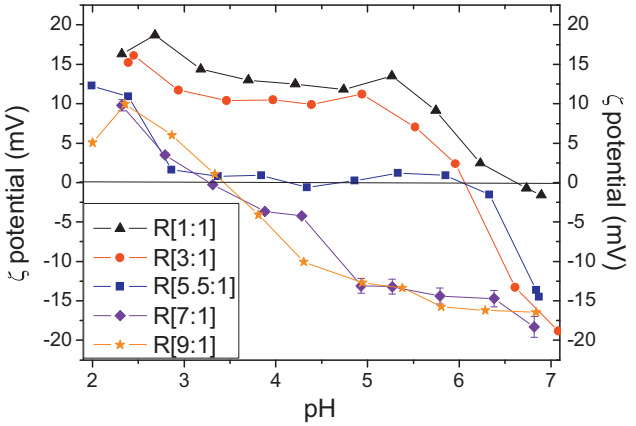


**Fig. 3.** pH dependence of ζ-potential of redispersed CC's at different $R_{[GA:Ch]}$: [1:1] (square), [3:1] (circle), [5.5:1] (triangle), [7:1] (diamond) and [9:1] (star).

were performed (Table 1). Several researches have shown that complex formation depends principally upon the concentrations, ratio and nature of the polyelectrolytes (charge, stiffness and spatial conformation), pH, ionic strength, order of mixing of reactants and rate of mixing (Espinosa-Andrews et al., 2007, 2010; Jiménez-Alvarado et al., 2009; Ramírez-Santiago et al., 2012; Schatz et al., 2004; Schmitt et al., 1999; Singh et al., 2007; Weinbreck et al., 2004). However, CC formation is a slow kinetic process and the rate and yield of CC is characteristic of each particular system. The spontaneous aggregation of the oppositely charged polyions takes place by electrostatic interaction upon mixing, forming aggregates of low configurational entropy, which rearrange to form the CC. Rearrangement occurs slowly, over hours or even days, and is driven by the gain in configurational entropy which occurs on the formation of a randomly mixed, concentrated coacervate phase and dilution of the aggregate phase (Burgess, 1990).

When the turbidity, $R_h$, and the absolute ζ-potential value of SC were lower, the CCY was higher, and this behavior is consistent with the fact that charge neutralization between -$COO^-$ and -$NH_3^+$ moieties was achieved. As seen in Table 1, for $R_{[GA:Ch]}$ in the range from $R_{[3:1]}$ to $R_{[5.5:1]}$ relatively higher CCY (Ec. 1) was obtained than at other $R_{[GA:Ch]}$ ratios. A similar behavior was observed for CC obtained from the interaction between medium molecular weight Ch and GA (Espinosa-Andrews et al., 2007). As the $R_{[GA:Ch]}$ moves further away from this range, the charge balance between both macromolecules also drifts further away from its stoichiometric mass ratio, CCY decreases and the turbidity of the SC increases.

The CC's were redispersed by putting them into acidic solution in order to determine the charge density of the system by adjusting the pH to different values (Fig. 3). The characteristics of CC's are mainly governed by the structural parameters of the individual biopolymers that make them up such as their charge density and chain length (Schatz et al., 2004). In general terms, all the curves displayed three distinct interaction zones: A) at low pH (~2) the biopolymers dispersions displayed positive charge density which decreased abruptly as pH was increased to a value of 3. At pH ~2.5 the glucosamine segments of Ch was completely protonized (Fig. 1), rendering the Ch molecules with a maximum positive charge density. At this same pH, the charge density of the GA molecules was almost nil due shielding of the carboxylic moieties by an excess of $H^+$ counterions. As the pH was increased to 3, the degree of protonation of Ch glucosamine segments remained more or less constant (Fig. 1), while the degree of ionization of the carboxylic groups in GA increased, so that the positive charges of Ch molecules began to form CC's with the negatively charged GA molecules; B) at intermediate pH values (~3–5) the CC's produced at $R_{[GA:Ch]}$ of [1:1], [3:1] and [5.5:1] tended to show a more or less constant charge region, while the CC's produced at $R_{[GA:Ch]}$ of [7:1] and [9:1] showed a continuous gain in negative charge density. At these pH values, both polymers are characterized by having only a fraction of their functional groups charged, which allows their molecular backbone to exhibit a relatively high degree of flexibility compared to their flexibility when fully charged or when completely uncharged. This flexibility permits more functional groups of both molecules to come into close contact and to interact electrostatically, and for a more balanced interaction to take place. This interaction is dependent on the biopolymers ratio. As shown in Fig. 1, Ch exhibited larger absolute charge density than GA, so that more molecules of GA are required for neutralizing the charge density of Ch molecules. That is why the charge density of the CC's was as follows: positive charged ([1:1] and [3:1]), neutral charged ([5.5:1]), and negative charged ([9:1] and [7:1]); and C) at relatively high pH values (>5) the CC's [1:1], [3:1] and [5.5:1] exhibited a sharp drop in ζ-potential values, which eventually resulted in a switchover from positive to negative values. As pH was increased from 5 to 7 the slight positive charge density of Ch molecules decayed to nil, while GA molecules achieved maximum degree of ionization and attained maximum negative charge density. This behavior was reflected in the rate of CC's formation in relation to biopolymers ratio. When the ζ-potential values close to zero for a given $R_{[GA:Ch]}$, a faster phase separation rate occurred, whereas relatively large ζ-potential values (positive or negative) resulted in relatively slow phase separation rate. Thus when GA was in excess in the $R_{[GA:Ch]}$, an insoluble complex devoid of charge was formed at a pH of ~6.2, whereas when Ch molecules were in excess in the $R_{[GA:Ch]}$ insoluble complex devoid of charge was formed at a pH of ~3.5.

### 3.3. Complex coacervate viscoelasticity

In order to understand the structural differences between of the CC's formed with different $R_{[GA:Ch]}$, their viscoelastic properties were determined at a pH value of 4.5 where the systems displayed the maximum charge difference (Fig. 1). All CC's exhibited similar profiles characterized by a LVER exhibiting a constant value for $G'$ and $G''$ up to a given strain %, followed by a sharp downward inflection in these moduli at larger strain % (data not show). The strain % where inflection occurs is indicative that CC structure breakdown commences and that the amount of stress that the CC can withstand before breakdown is evidenced by the shift in the inflection point (Lobato-Calleros, Rodríguez, Sandoval-Castilla, Vernon-Carter, & Alvarez-Ramirez, 2006). In this work

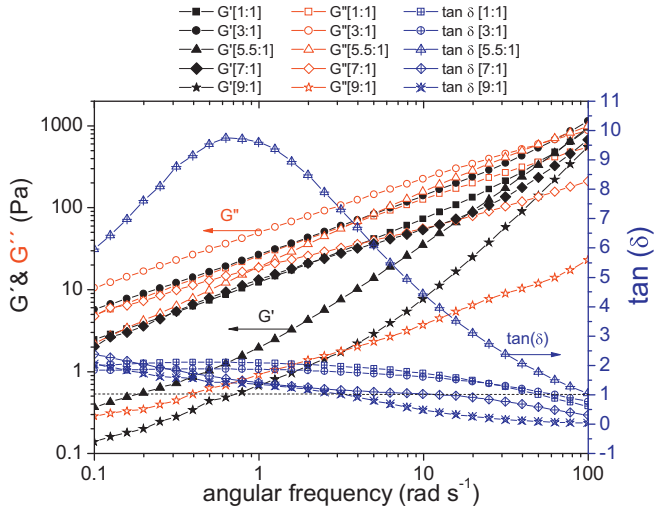


**Fig. 4.** Oscillation frequency ($\omega$) sweep of complex coacervates obtained at different biopolymers mass ratio $R_{[GA:Ch]}$ at 5 °C: [1:1] (square), [3:1] (circle), [5.5:1] (triangle), [7:1] (diamond) and [9:1] (star). Values of $G'$ (filled symbols), $G''$ (empty symbols) and tan $\delta$ (cross symbols).

the inflection point was shifted to the right for $R_{[5.5:1]}$ to about a strain % of 65, but as the $R_{[GA:Ch]}$ decreased or increased, it shifted to the left. Lower $R_{[GA:Ch]}$, i.e. those where Ch was in excess ([1:1] and [3:1]) and displayed a positive charge density, showed LVER up to a strain % of ~20. Lowest LVER was observed for $R_{[7:1]}$ and $R_{[9:1]}$, where GA was in excess and relatively high negative charge occurred, merely reaching a strain % value of under ~2. Espinosa-Andrews et al. (2010) reported that the viscoelastic behavior of CC's was closely related to a sponge-like microstructure of the coacervate that resulted from a highly cross-linked compact network entrapping water molecules within vacuoles of different size, whose distributions were affected by pH values.

Fig. 4 shows the variation of $G'$ and $G''$ with angular frequency ($\omega$) sweep for the CC's obtained from different $R_{[GA:Ch]}$. At low frequencies (in the range of 0.1–2) $G''$ was higher than $G'$, indicative that all CC's exhibited liquid-viscoelastic behavior. All of the CC's exhibited a crossover between $G''$ and $G'$ at higher $\omega$, with the gel point shifting higher $\omega$ values as follows: the $R_{[9:1]} < R_{[7:1]} < R_{[1:1]} < R_{[3:1]} < R_{[5.5:1]}$. These results pinpoint that stronger interactions occur between CC's molecules when gel points are reached at higher $\omega$ values. This fact seems to be confirmed by the $R_h$ values exhibited by the SC (Table 1). Lower $R_h$ values give rise to stronger interactions between CC's molecules. At $R_{[5.5:1]}$ where CC's are devoid of charge, interactions between CC's molecules are mainly due to strong polymer-polymer interactions (including hydrophobic interactions). On the other hand, in the $R_{[9:1]}$ where a large negative charge density exists, CC molecules are extended and interactions between neighboring molecules occur predominantly by physical entanglement and by electrostatic interactions, which are weaker than hydrophobic bonds (McClements, 2005). Tan $\delta$ of the CC's obtained from different $R_{[GA:Ch]}$ exhibited the same order than that corresponding to the gel point, result that corroborates our hypothesis exposed above.

## 4. Conclusions

In light of these results, it seems than an interrelationship exists between the biopolymers mass ratio, charge density and the viscoelastic properties of the complex coacervate phases. To this respect, the complex coacervate obtained at a biopolymers mass ratio of [5.5:1] was the one in which stronger interactions, smaller hydrodynamic radius and lowest zeta potential values occurred. As the biopolymers mass ratio drifted further away from a [5.5:1] ratio, zeta potential and hydrodynamic radius values increased, but increasingly weaker interactions took place between complex coacervate molecules, resulting in lower viscoelastic properties and the establishment of gel point at lower angular frequencies. This study provides useful information for obtaining new biomaterials by complex coacervation of biopolymers with differing rheological properties.

## Acknowledgment

We would like to thank the Consejo Nacional de Ciencia y Tecnología de México (CONACyT) for financing this study through grant CB-2008-01-104109.

## References

Burgess, D. J. (1990). Practical analysis of complex coacervate systems. *Journal of Colloid and Interface Science*, *140*(1), 227–238.
Claesson, P. M., & Ninhami, B. W. (1992). pH dependent interactions between adsorbed chitosan layers. *Langmuir*, *8*, 1406–1412.
Dickinson, E. (1995). Emulsion stabilization by polysaccharides and protein polysaccharide complexes. In A. M. Stephen (Ed.), *Food polysaccharides and their applications* (pp. 501–515). New York: Marcel Dekker.
Espinosa-Andrews, H., Sandoval-Castilla, O., Vázquez-Torres, H., Vernon-Carter, E. J., & Lobato-Calleros, C. (2010). Determination of the gum Arabic–chitosan interactions by Fourier Transform Infrared Spectroscopy and characterization of the microstructure and rheological features of their coacervates. *Carbohydrate Polymers*, *79*, 541–546.
Espinosa-Andrews, H., Báez-González, J. G., Cruz-Sosa, F., & Vernon-Carter, E. J. (2007). Gum Arabic–chitosan complex coacervation. *Biomacromolecules*, *8*(4), 1313–1318.
Espinosa-Andrews, H., Lobato-Calleros, C., Loeza-Corte, J. M., Beristain, C. I., Rodríguez-Huezo, M. E., & Vernon-Carter, E. J. (2008). Quantification of the composition of gum arabic–chitosan coacervates by HPLC. *Revista Mexicana de Ingeniería Química*, *7*(3), 293–298.
Guzey, D., & McClements, D. J. (2006). Characterization of b-lactoglobulin–chitosan interactions in aqueous solutions: A calorimetry, light scattering, electrophoretic mobility and solubility study. *Food Hydrocolloids*, *20*, 124–131.
Helgason, T., Gislason, J., McClements, D. J., Kristbergsson, K., & Weiss, J. (2009). Influence of molecular character of chitosan on the adsorption of chitosan to oil droplet interfaces in an in vitro digestion model. *Food Hydrocolloids*, *23*, 2243–2253.
Hernández-Ochoa, L., Gonzales-Gonzales, A., Gutiérrez-Mendez, N., Muñoz-Castellanos, L. N., & Quintero-Ramos, A. (2011). Study of the antibacterial activity of chitosan-based films prepared with different molecular weights including spices essential oils and functional extracts as microbial agents. *Revista Mexicana de Ingenieria Quimica*, *10*, 455–463.
Hudson, S. M., & Jenkins, D. W. (2001). Chitin and chitosan. In: Encyclopedia of polymer science and technology (574 pp.).
Jiménez-Alvarado, R., Beristain, C. I., Medina-Torres, L., Román-Guerrero, A., & Vernon-Carter, E. J. (2009). Ferrous bisglycinate content and release in $W_1/O/W_2$ multiple emulsions stabilized by protein–polysaccharide complexes. *Food Hydrocolloids*, *23*(8), 2425–2433.
Klinkesorn, U., & Namatsila, Y. (2009). Influence of chitosan and NaCl on physicochemical properties of low-acid tuna oil-in-water emulsions stabilized by non-ionic surfactant. *Food Hydrocolloids*, *23*, 1374–1380.
Liu, S., Low, N. L., & Nickerson, M. T. (2010). Effect of pH, salt, and biopolymer ratio on the formation of pea protein isolate-gum arabic complexes. *Carbohydrate Polymers*, *79*, 541–546.
Lobato-Calleros, C., Rodríguez, E., Sandoval-Castilla, O., Vernon-Carter, E. J., & Alvarez-Ramirez, J. (2006). Reduced-fat white fresh cheese-like products obtained from W1/O/W2 double emulsions: Viscoelastic and high-resolution image analyses. *Food Research International*, *39*, 678–685.
McClements, D. J. (2005). *Food emulsions: Principles, practice and techniques* (2nd ed.). Boca Raton: CRC Press. (Chapter 3).
Niederhofer, A., & Müller, B. W. (2004). A method for direct preparation of chitosan with low molecular weight from fungi. *European Journal of Pharmaceutics and Biopharmaceutics*, *57*, 101–105.
Park, J. H., Saravanakumar, G., Kim, K., & Kwon, I. C. (2010). Targeted delivery of low molecular drugs using chitosan and its derivatives. *Advanced Drug Delivery Reviews*, *62*(1), 28–41.
Pérez-Orozco, J. P., Barrios-Salgado, E., Román-Guerrero, A., & Pedroza-Islas, R. (2011). Interaction of mesquite gum–chitosan at the interface and its influence on the stability of multiple emulsions $W_1/O/W_2$. *Revista Mexicana de Ingenieria Quimica*, *10*, 487–499.
Ramírez-Santiago, C., Lobato-Calleros, C., Espinosa-Andrews, H., & Vernon-Carter, E. J. (2012). Viscoelastic properties and overall sensory acceptability of reduced-fat

Petit-Suisse cheese made by replacing milk fat with complex coacervate. *Dairy Science & Technology*, *92*, 383–398.
Renard, D., Lavenant-Gourgeon, L., Ralet, M. C., & Sanchez, C. (2006). Acacia senegal gum: Continuum of molecular species differing by their protein to sugar ratio, molecular weight, and charges. *Biomacromolecules*, *7*, 2637–2649.
Schatz, C., Lucas, J. M., Viton, C., Domard, A., Pichot, C., & Delair, T. (2004). Formation and properties of positively charged colloids based on polyelectrolyte complexes of biopolymers. *Langmuir*, *20*, 7766–7778.
Schmitt, C., Sanchez, C., Thomas, F., & Hardy, J. (1999). Complex coacervation between b-lactoglobulin and acacia gum in aqueous medium. *Food Hydrocolloids*, *13*, 483–496.
Semenova, M. G. (2007). Thermodynamic analysis of the impact of molecular interactions on the functionality of food biopolymers in solution and in colloidal systems. *Food Hydrocolloid*, *21*, 23–45.
Singh, S. S., Siddhanta, A. K., Meenab, R., Prasad, K., Bandyopadhyay, S., & Bohidar, H. B. (2007). Intermolecular complexation and phase separation in aqueous solutions of oppositely charged biopolymers. *International Journal of Biological Macromolecules*, *41*, 185–192.
Walstra, P. (2003). Physical chemistry of food. In P. Walstra (Ed.), *Polymers* (pp. 179–187). New York-Basel: Marcel Dekker, Inc.
Weinbreck, F., Tromp, R. H., & de Kruif, C. G. (2004). Composition and structure of whey protein/gum arabic coacervates. *Biomacromolecules*, *5*, 1437–1445.